Figure S1

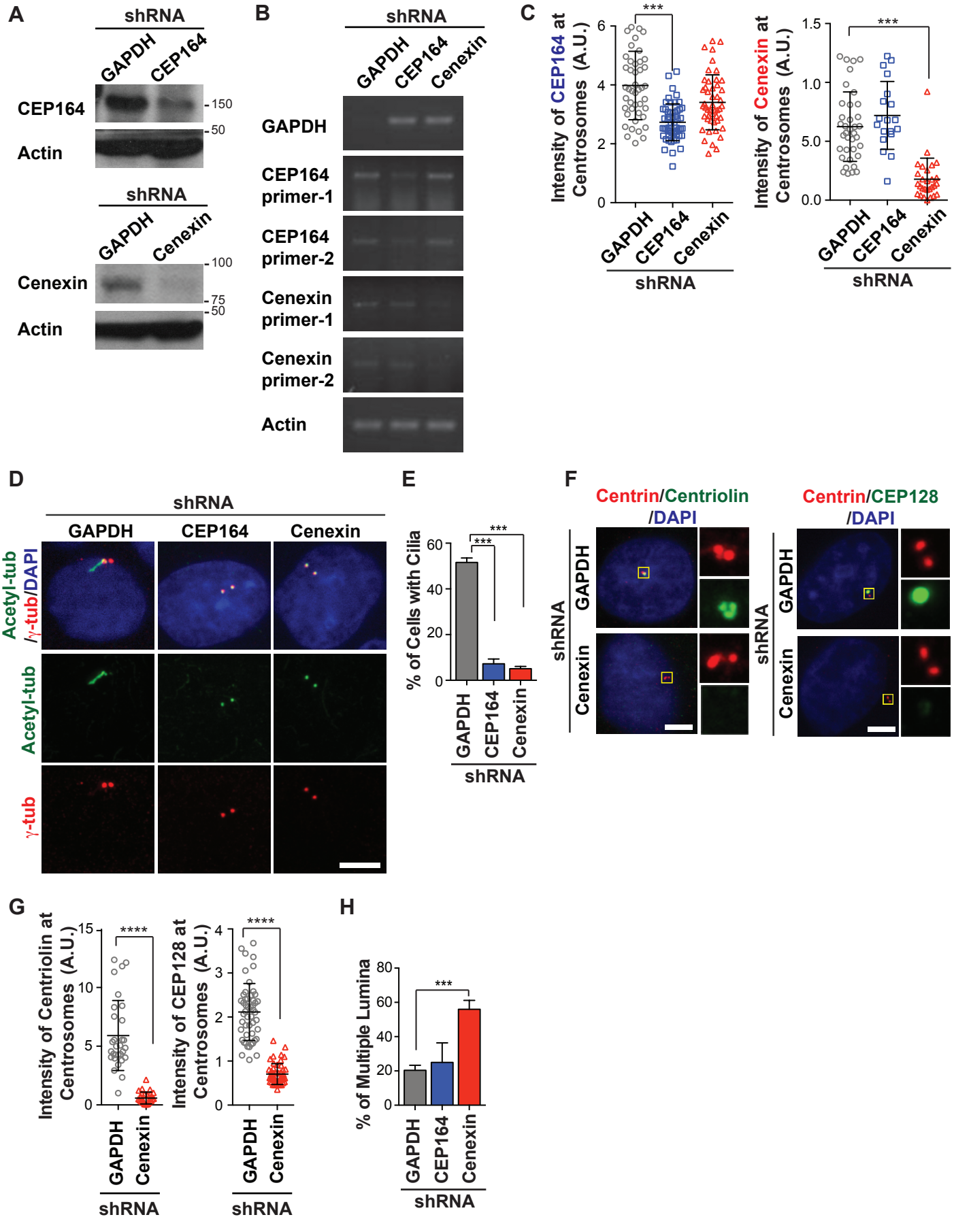
A
shRNA
GAPDH
CEP164
CEP164
150
50
Actin
shRNA
GAPDH
Cenexin
Cenexin
100
75
50
Actin
B
shRNA
GAPDH
CEP164
Cenexin
GAPDH
CEP164 primer-1
CEP164 primer-2
Cenexin primer-1
Cenexin primer-2
Actin
C
Intensity of CEP164 at Centrosomes (A.U.)
***
GAPDH
CEP164
Cenexin
shRNA
Intensity of Cenexin at Centrosomes (A.U.)
***
GAPDH
CEP164
Cenexin
shRNA
D
shRNA
GAPDH
CEP164
Cenexin
Acetyl-tub/γ-tub/DAPI
Acetyl-tub
γ-tub
E
% of Cells with Cilia
***
***
GAPDH
CEP164
Cenexin
shRNA
F
Centrin/Centriolin /DAPI
Centrin/CEP128 /DAPI
shRNA
GAPDH
Cenexin
G
Intensity of Centriolin at Centrosomes (A.U.)
****
GAPDH
Cenexin
shRNA
Intensity of CEP128 at Centrosomes (A.U.)
****
GAPDH
Cenexin
shRNA
H
% of Multiple Lumina
***
GAPDH
CEP164
Cenexin
shRNA

Figure S2

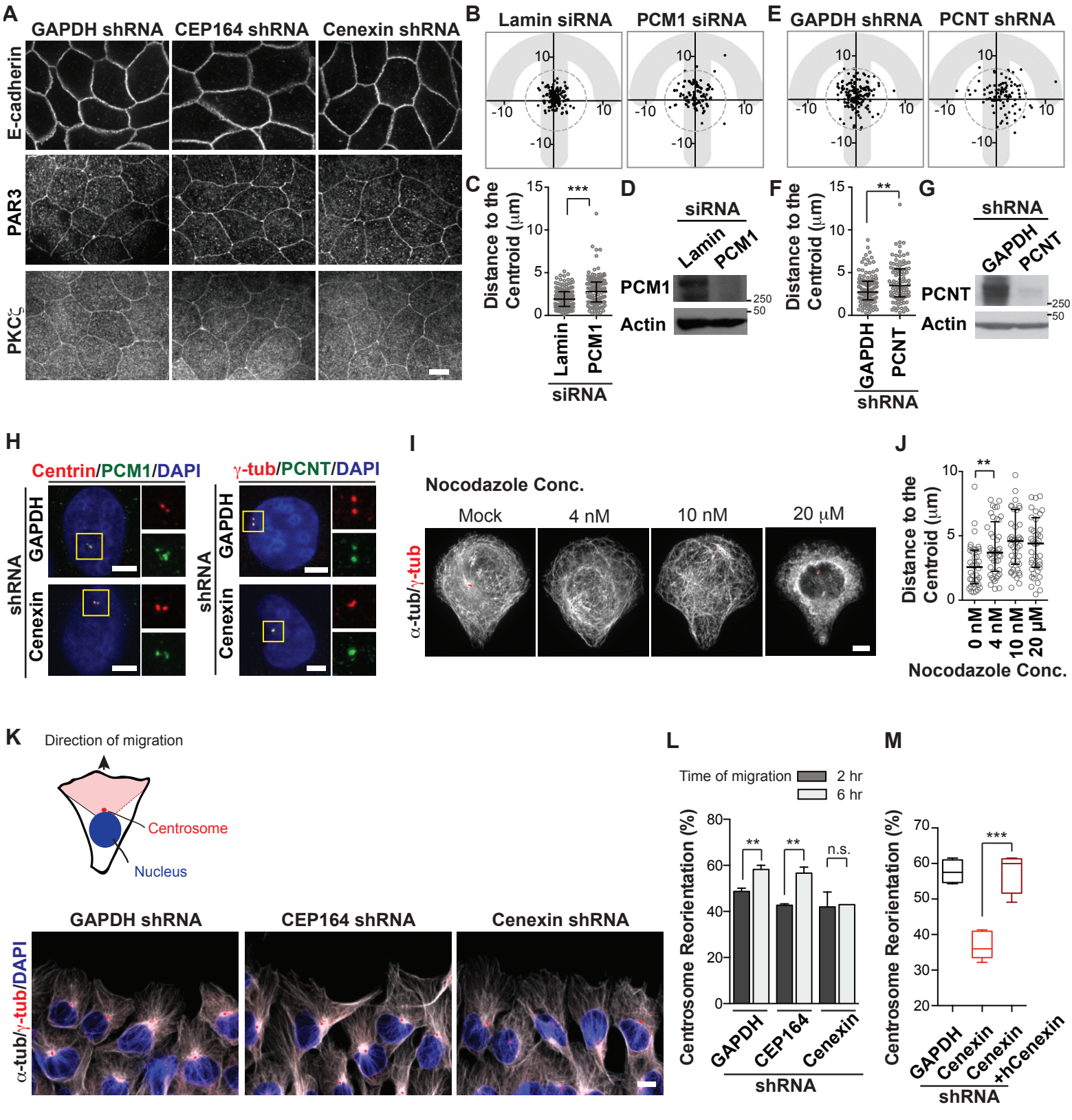
A
GAPDH shRNA
CEP164 shRNA
Cenexin shRNA
E-cadherin
PAR3
PKCζ
B
Lamin siRNA
PCM1 siRNA
E
GAPDH shRNA
PCNT shRNA
C
Distance to the Centroid (μm)
***
Lamin
PCM1
siRNA
D
siRNA
Lamin
PCM1
PCM1
Actin
250
50
F
Distance to the Centroid (μm)
**
GAPDH
PCNT
shRNA
G
shRNA
GAPDH
PCNT
PCNT
Actin
250
50
H
Centrin/PCM1/DAPI
γ-tub/PCNT/DAPI
shRNA
GAPDH
Cenexin
I
Nocodazole Conc.
Mock
4 nM
10 nM
20 μM
α-tub/γ-tub
J
Distance to the Centroid (μm)
**
0 nM
4 nM
10 nM
20 μM
Nocodazole Conc.
K
Direction of migration
Centrosome
Nucleus
GAPDH shRNA
CEP164 shRNA
Cenexin shRNA
α-tub/γ-tub/DAPI
L
Time of migration
2 hr
6 hr
Centrosome Reorientation (%)
**
**
n.s.
GAPDH
CEP164
Cenexin
shRNA
M
Centrosome Reorientation (%)
***
GAPDH
Cenexin
Cenexin
+hCenexin
shRNA

Figure S3

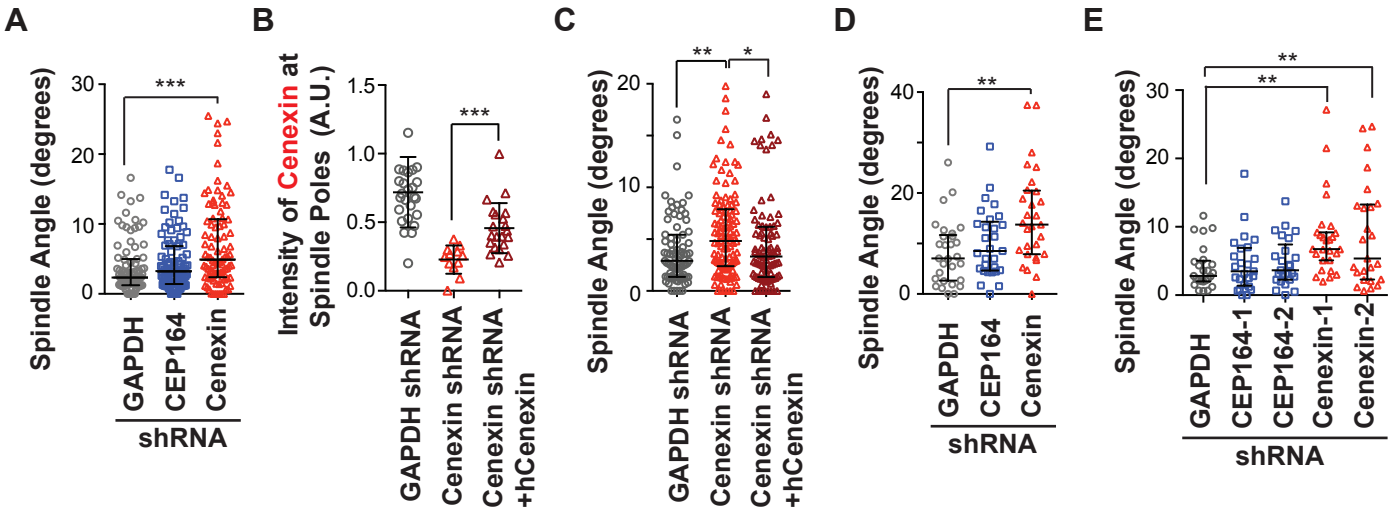
A
Spindle Angle (degrees)
30
20
10
0
***
GAPDH
CEP164
Cenexin
shRNA
B
Intensity of Cenexin at Spindle Poles (A.U.)
1.5
1.0
0.5
0.0
***
GAPDH shRNA
Cenexin shRNA
Cenexin shRNA +hCenexin
C
Spindle Angle (degrees)
20
10
0
**
*
GAPDH shRNA
Cenexin shRNA
Cenexin shRNA +hCenexin
D
Spindle Angle (degrees)
40
20
0
**
GAPDH
CEP164
Cenexin
shRNA
E
Spindle Angle (degrees)
30
20
10
0
**
**
GAPDH
CEP164-1
CEP164-2
Cenexin-1
Cenexin-2
shRNA

Figure S4

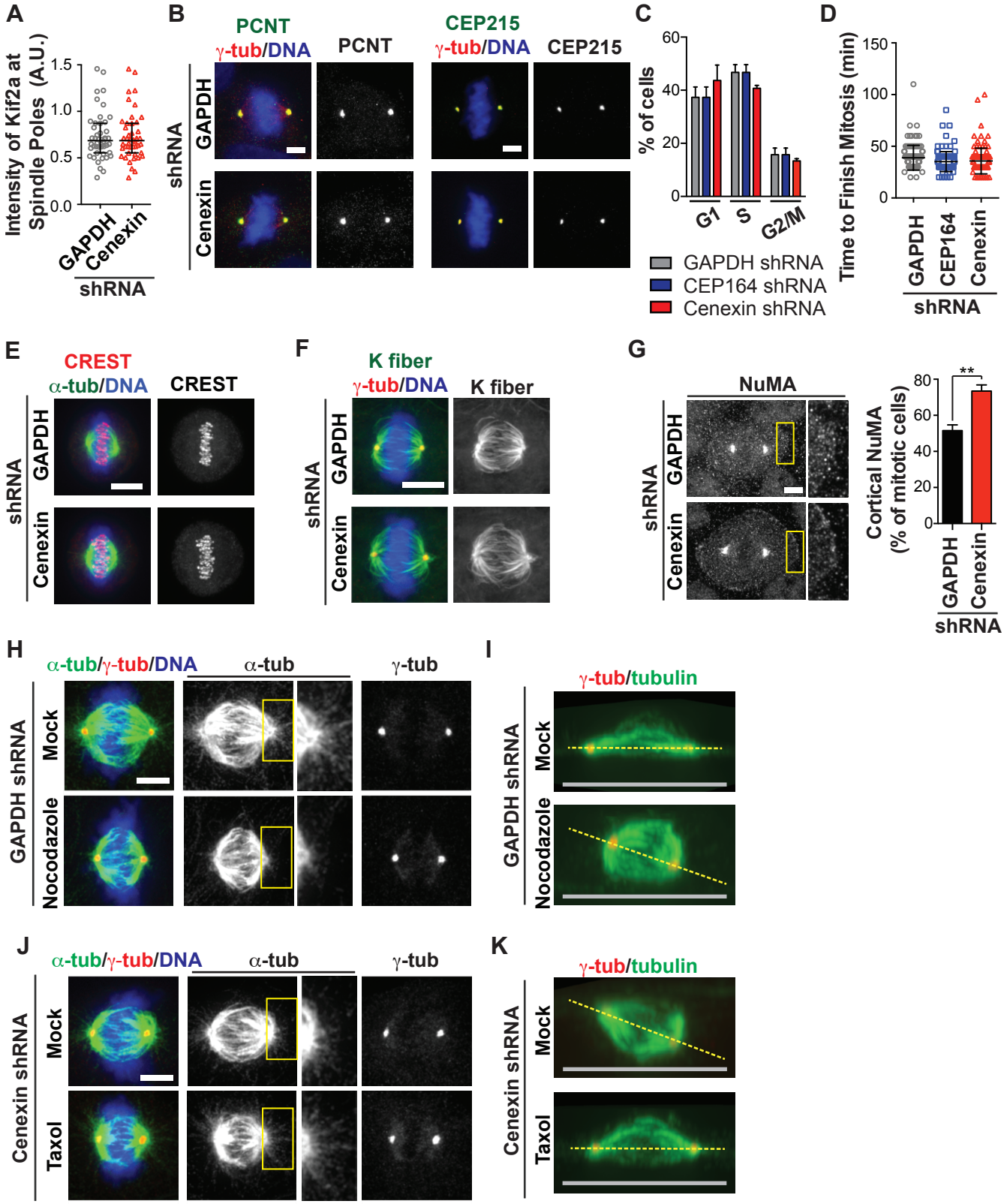
A
Intensity of Kif2a at Spindle Poles (A.U.)
1.5
1.0
0.5
0.0
GAPDH
Cenexin
shRNA
B
PCNT
γ-tub/DNA
PCNT
CEP215
γ-tub/DNA
CEP215
shRNA
GAPDH
Cenexin
C
% of cells
60
40
20
0
G1
S
G2/M
GAPDH shRNA
CEP164 shRNA
Cenexin shRNA
D
Time to Finish Mitosis (min)
150
100
50
0
GAPDH
CEP164
Cenexin
shRNA
E
CREST
α-tub/DNA
CREST
shRNA
GAPDH
Cenexin
F
K fiber
γ-tub/DNA
K fiber
shRNA
GAPDH
Cenexin
G
NuMA
shRNA
GAPDH
Cenexin
Cortical NuMA (% of mitotic cells)
80
60
40
20
0
**
GAPDH
Cenexin
shRNA
H
α-tub/γ-tub/DNA
α-tub
γ-tub
GAPDH shRNA
Mock
Nocodazole
I
γ-tub/tubulin
GAPDH shRNA
Mock
Nocodazole
J
α-tub/γ-tub/DNA
α-tub
γ-tub
Cenexin shRNA
Mock
Taxol
K
γ-tub/tubulin
Cenexin shRNA
Mock
Taxol

Supplemental Figure Legends

Figure S1 (Related to Figure 1).
(A) Immunoblot analysis of U2OS cells treated with CEP164 shRNA (upper images) or cenexin shRNA (lower images), and compared to cells treated with control shRNA (GAPDH). Staining with antibodies to actin (loading control), and CEP164 (top) or cenexin (bottom). See also Figure 1B-1D.
(B) RT-PCR analysis showing CEP164 and cenexin gene expression in MDCK cells depleted of GAPDH (control), CEP164 or cenexin.
(C) The integrated intensity of CEP164 (left) or cenexin (right) at centrosomes measured in MDCK cells depleted of GAPDH, CEP164 and cenexin. Data are represented as mean ± SD of >20 centrosomes in each group. ***, *p*-value <0.001. See also Figure S1B.
(D-E) MDCK cells treated with shRNAs targeting CEP164 or cenexin were defective in ciliogenesis when compared to control (GAPDH shRNA). Cells were seeded at confluence on 0.4 mm transmembrane and cultured in serum-free conditions for 5 days. Cells were fixed with cold methanol and stained for cilia (acetylated tubulin, green), centrosomes (γ-tubulin, red), and nuclei (DAPI, blue). Scale bar, 5 μm.
(E) The percentage of cells having cilia was calculated for n=3 experiments. Data are represented as mean ± SD. >50 cells were counted in each group. ***, *p*-value <0.001.
(F) The subdistal appendage proteins, centriolin (left) and CEP128 (right) at interphase centrosomes were displaced from the mother centrioles in cenexin-depleted U2OS cells. Centrosomes were stained for centrin (red), centriolin or CEP128 (green), and nuclei (DAPI, blue). Insets depict 4.5x magnification of the centrosome region. Scale bar, 5 μm.
(G) The integrated intensity of centriolin (left) or CEP128 (right) at centrosomes measured in U2OS cells depleted of GAPDH and cenexin. Data are represented as mean ± SD of >30 centrosomes in each group. ****, *p*-value <0.0001.
(H) The percentage of acini with >1 lumen in MDCK 3-D cultured cells depleted of GAPDH, CEP164, or cenexin. Data are represented as mean ± SD from 3 independent experiments. >30 acini were counted in each group per experiment. ***, *p*-value <0.001.

Figure S2 (Related to Figure 2).
(A) Depletion of CEP164 or cenexin did not affect localization of E-cadherin (top row), PAR3 (middle row), and PKCζ (bottom row) in polarized MDCK cultures. Cells were grown on transwell membranes (0.4 μm pore size) for 5 days under serum-free conditions. Scale bar, 10 μm.
(B) Interphase centrosome positions for >125 centrosomes are plotted for lamin-depleted (control) and PCM1-depleted U2OS cells using a previously published siRNA [S1].
(C) Distances between centrosomes and the cell centroid (shown in Figure S2B) are shown for lamin- and PCM1-depleted cells. Data are represented as median ± interquartile range. ***, *p*-value<0.001.
(D) Immunoblot analysis of U2OS whole cell lysates after cells were treated with control or PCM1 siRNA. Staining against PCM1 and actin (loading control) is shown.
(E) Interphase centrosome positions were measured from cells grown on crossbow micropattern slides. 164 centrosomes were plotted for the control cells (GAPDH-depleted), and 99 centrosomes for PCNT-depleted U2OS cells.
(F) Distances between the scored centrosomes and the cell centroid (shown in Figure S2E) for GAPDH- and PCNT-depleted cells were measured. Data are represented as median ± interquartile range. **, *p*-value<0.01.
(G) Immunoblot analysis of U2OS whole cell lysate treated with PCNT or control (GAPDH) shRNA. Staining with antibodies against PCNT and actin.
(H) The presence of PCM1 or PCNT at interphase centrosomes was not decreased in cenexin-depleted U2OS cells. Cells were stained for centrosomes (centrin or γ-tubulin, red), and PCM1 or PCNT (green). Insets depict 2x magnification of the centrosome region. Scale bar, 5 μm.
(I) As in Figure 2A, U2OS cells were grown on crossbow micropatterned slides and treated with nocodazole (mock, 4 nM, 10 nM, and 20 mM), and stained for microtubules (α-tubulin, white) and centrosomes (γ-tubulin, red). Scale bar, 10 μm.
(J) Distances between centrosomes and the cell centroid with various nocodazole treatments. Data are represented as median ± interquartile range of >50 cells/treatment. Representative of n=2 experiments. **, *p*-value <0.01.

(K) Top row, a model depicting centrosome (red) localization during migration. Upon inducing cell migration, the centrosome reorients into the light red quadrant in front of the nucleus (blue) towards the direction of migration. Bottom row, U2OS cells depleted of GAPDH (control), CEP164, or cenexin were fixed and stained for centrosomes (γ-tubulin, red), nuclei (DAPI, blue), and microtubules (α-tubulin, white) 6-hours after scratch wound application. Scale bar, 10 μm.
(L) The percentage of centrosomes that orient towards the front quadrant (modeled in S4K, top row, light red section) at 2 hours (dark grey) and 6 hours (light grey) after scratch wound application. Cells were depleted of GAPDH, CEP164, or cenexin. Data are represented as mean ± SEM for 3 independent experiments, and >200 cells were counted in each group/experiment. **, p-value<0.01. n.s. = not significant.
(M) U2OS cells depleted of GAPDH or cenexin, and subsequently rescued with an shRNA-resistant human cenexin were scored for centrosome reorientation towards the leading edge 6-hours after scratch wound application. Data are represented as a box-and-whisker plot with max and min of >300 cells over 3 regions in each group. Representative of n=2 experiments. ***, p-value<0.001.

Figure S3 (Related to Figure 3).
(A) Collective raw spindle angles from Figure 3F are shown. Data are represented as median ± interquartile range. ***, p-value <0.001.
(B) MDCK cells treated with GAPDH shRNA, cenexin shRNA, or cenexin shRNA plus an shRNA-resistant human cenexin construct were fixed and stained for cenexin. The integrated intensity of cenexin at mitotic spindle poles was measured for each treatment. Each dot represents the average intensity of two spindle poles in the cell, and mean ± SD is shown. >20 cells were measured for each group. ***, p-value <0.001.
(C) Collective raw spindle angles were measured and compared between MDCK cells depleted of cenexin and cells rescued with an shRNA resistant cenexin (Figure 3H). Data are represented as median ± interquartile range. *, p-value<0.05. **, p-value<0.01.
(D) Demonstrates the raw spindle angles measured in U2OS cells depleted of GAPDH, CEP164, or cenexin. Data are represented as median ± interquartile range of 29 cells. **, p-value<0.01.
(E) Raw spindle angles were measured in MDCK cells treated with a GAPDH shRNA, and two different shRNAs towards either CEP164, or cenexin. CEP164-1 and cenexin-1 shRNAs were the same shRNAs used in Figure 3E-3H. CEP164-2 and cenexin-2 shRNAs were additional shRNAs to confirm the protein depletion phenotype. Data are represented as median ± interquartile range. A representative of n=3 experiments is shown, n=25 cells/treatment. **, p-value<0.01.

Figure S4 (Related to Figure 4).
(A) The integrated intensity of Kif2a at spindle poles was measured for GAPDH-, and cenexin-depleted MDCK cells. Data are represented as mean ± SD of 46 poles in each group. See Figure 4B.
(B) The presence of PCNT (left) or CEP215 (right) at spindle poles was unchanged in cenexin-depleted U2OS cells. Spindle pole (γ-tubulin, red), PCNT or CEP215 (green). Scale bar, 5 μm.
(C) Cell cycle distribution was analyzed by propidium iodide (PI) staining and flow cytometry in MDCK cells depleted of GAPDH, CEP164, or cenexin. $2x10^4$ cells were analyzed in each group. The average percentage of cells at G1, S-phase, and G2/M are represented ± SD from 3 experiments.
(D) Time-lapse imaging was used to determine prophase to cytokinesis duration in MDCK cells depleted of GAPDH, CEP164, or cenexin. 100 cells were recorded in each group. Mean ± SD are shown.
(E) Cenexin-depletion does not affect chromosome congression during mitosis. Cells were stained for kinetochore (CREST, red), the mitotic spindle (α-tubulin, green), and DNA (DAPI, blue). Scale bar, 5 μm.
(F) Cenexin depletion does not affect kinetochore fibers in mitotic spindles. MDCK cells were placed on ice for 20 minutes before fixing. Cells were stained for kinetochore fibers (K fiber; α-tubulin, green), centrosomes (γ-tubulin, red), and DNA (DAPI, blue). Scale bar, 5 μm.
(G) Cenexin-depletion causes NuMA mislocalization at the cell cortex in MDCK cells. Left, a single z-section is shown for metaphase MDCK cells depleted of GAPDH or cenexin were stained for NuMA. Scale bar, 5 μm. Insets taken from yellow box were magnified 2x to illustrate the increase in cortical NuMA with cenexin-loss compared to control (GAPDH-depleted cell). Right, the percentage of mitotic cells with visible cortical NuMA localization in MDCK cells treated with cenexin- or GAPDH-shRNAs. Mean ± SEM. 30 cells/treatment were counted per n=3 experiments. **, p-value<0.01.

(H) Astral microtubules were disrupted with nocodazole treatment in control (GAPDH shRNA) U2OS cells, while the spindle and spindle poles were kept intact. Cells were fixed and stained for microtubules (α-tubulin, green), spindle poles (γ-tubulin, red), and DNA (DAPI, blue). Insets taken from yellow box were magnified 2x. Scale bar, 5 μm. See also Figure 4G.
(I) Orthogonal view of metaphase U2OS cells treated with nocodazole, fixed, and stained for microtubules (a-tubulin, green), and spindle poles (γ-tubulin, red). See Figure 4K.
(J) Cenexin-depleted U2OS cells treated with taxol demonstrated an increase in astral microtubules. Cells were fixed and stained for microtubules (α-tubulin, green), spindle poles (γ-tubulin, red), and DNA (DAPI, blue). Insets taken from yellow box were magnified 2x. Scale bar, 5 μm. See also Figure 4H.
(K) Orthogonal view of metaphase U2OS cells depleted of cenexin treated with taxol. Cells were fixed and stained for microtubules (α-tubulin, green), and spindle poles (γ-tubulin, red). See also Figure 4K.

Supplemental Experimental Procedures

Materials

The following primary antibodies were used for immunofluorescence staining or immunoblotting: rabbit anti-cenexin (Abcam and Proteintech), rabbit anti-CEP164 (from Dr. Erich Nigg, University of Basel, and Novus), goat anti-γ-tubulin (Santa Cruz), mouse anti-centrin (EMD Millipore), rat anti-α-tubulin (EMD Millipore), mouse anti-acetylated tubulin (Sigma-Aldrich), rabbit anti-NuMA (Abcam), mouse anti-E-cadherin (BD Biosciences), rabbit anti-PAR3 (EMD Millipore), rabbit anti-PKCζ (Santa Cruz), rabbit anti-pericentrin (Abcam), rabbit anti-CEP215 (Bethyl Laboratories). The following secondary antibodies were used for immunofluorescence staining: donkey anti-goat 568 (Invitrogen), donkey anti-rat DyLight 649, donkey anti-rabbit Alexa 647, donkey anti-mouse Alexa 647, donkey anti-rabbit Alexa 488, donkey anti-mouse DyLight 488 (Jackson ImmunoResearch Group). Nocodazole, taxol, and cytochalasin D were obtained from Sigma-Aldrich. GAPDH, cenexin (cenexin-1: V3LMM 507347; cenexin-2: V3LHS 336238, [S2]), CEP164 (CEP164-1: V2LHS 96265; CEP164-2: V2LHS 232472), and pericentrin (V3LHS 368782) shRNAs were purchased from Open Biosystems (GE Dharmacon) and the UMMS RNAi Core Facility generated lentivirus for each. Human cenexin-GFP construct was from Dr. Kyung S Lee, National Cancer Institute [S3], and we introduced two mutations on nucleotide 783-784 (AC➔GT) so that it was resistant to shRNA silencing.

Cell lines and culture

U2OS and MDCK cells were grown in Dulbecco's Modified Eagle Medium (Invitrogen) supplemented with 10% fetal bovine serum (Atlanta Biologicals) and 100 U/ml Penicillin-Streptomycin (Gibco). To establish cell lines depleted of a specific protein, lentiviruses expressing target gene shRNAs were incubated with cells for 24 hours in the presence of 4 μg/ml polybrene (Sigma). Puromycin (3 μg/ml) was used to select for transduced cells. The crossbow micropattern slides were from CYTOO (Mini CW-S-FN).

Nocodazole (M1401; Sigma) and taxol (T7191 and T7402; Sigma) were dissolved in DMSO. For nocodazole treatment, unless otherwise specified, the concentration of nocodazole was 100 nM. For taxol treatment, we titrated the working concentration by checking if it caused multiple spindle defects in mitosis. The working concentration that was used in Figure 2-4 was 5-50 nM. For centrosome centering experiments with micropatterned slides in Figure 2, cells were seeded onto patterned slides and incubated for 2 hours for cell attachment. Cells were further incubated with nocodazole or taxol in serum-free medium for 2 hours before immunofluorescence staining.

Reverse transcription (RT-PCR) analysis

Total RNA was isolated from cells by using TRIzol reagent (Ambion), and 5 μg of RNA was converted into 100 μl of cDNA by using SuperScript II RT kit (Invitrogen). The following PCR primers were used to detect gene expression in MDCK cells: Actin, forward 5'-CAA AGC CAA CCG TGA GAA G-3', reverse 5'-CAG AGT CCA TGA CAA TAC CAG-3'; GAPDH, forward 5'-AAC ATC ATC CCT GCT TCC AC-3', reverse 5'-GAC CAC CTG GTC CTC AGT GT-3'; cenexin primer-1, forward 5'-GCA TGT GCA ACT TGC TGA CA-3', reverse 5'-TTC AGG ATG TCA GGC AGC TG-3'; cenexin primer-2, forward 5'-CAA CAT CGA GCG CAT CAA GG-3', reverse 5'-GCT CAG CTT CTG CAG GAG AA-3'; CEP164 primer-1, forward 5'-GAC CCC CAA GTC TCA GGT TG-3', reverse 5'-TTG TAT GCA GTG GAG AGG CG-3'; CEP164 primer-2, forward 5'-CCT GGA TGA GGC AGC ATT GA-3', reverse 5'-AGT CAG CAG AGG GAG GAG AG-3'.

Immunofluorescence staining

Cells were seeded on glass coverslips (#1.5, Warner Instruments) and grown to sub-confluence for immunofluorescence confocal microscopy. Cells were then fixed (cold methanol) and stained as previous described [S2, S4–S6]. Images were taken on a Perkin Elmer spinning disk confocal microscope: Zeiss Axiovert 200, Plan-Apochromat 100x/1.4 Oil DIC objective and Hamamatsu ORCA-ER camera. The entire cell was imaged at 0.2-μm step-intervals and displayed as maximum projections (MetaMorph, Molecular Device) unless otherwise specified. The fluorescence range of intensity was adjusted identically for each image series. For immunofluorescence staining of isolated centrosomes, centrosomes were prepared and stained according to our previous studies [S2, S7, S8]. For fluorescence intensity quantification at centrosomes/spindle poles, the integrated intensity was measured using a sum projection of the original

stack followed by previously described methods [S4, S6]. The quantification of CEP128 (Figure S1F) was performed using maximum projections of the original stack due to a high degree of background staining. Orthogonal images of mitotic spindle were processed with Imaris software. For measuring spindle angles in 2-dimensional cultures, γ-tubulin staining was used to indicate spindle pole positions, and spindle angle measurements were carried out as previous described [S4–S6]. For measuring astral microtubule length by EB1 staining, Imaris software was used followed by a previously described method [S9].

Three-dimensional acinus culture and staining

Modified from previously published methods [S10]. MDCK cells were seeded in 2% matrigel (BD Biosciences) at 5 x 10^3 cells per well on matrigel pre-coated 8-well chamber slides (Thermo Scientific Nunc). After 36 to 48 hours, acini were fixed with 4% paraformaldehyde for 20 minutes, and permeablized with 0.5% Triton X-100 for 10 minutes at 4°C. Before blocking with 10% donkey serum for 2 hours, acini were rinsed with PBS twice. To stain target proteins, acini were incubated with primary antibodies overnight at 4°C. Acini were rinsed three times with PBS for 20 minutes each at room temperature and then incubated with rhodamine phalloidin or secondary antibodies for 1 hour. After a brief wash with PBS, acini were stained with DAPI and mounted in ProLong Gold Antifade reagent (Invitrogen). Images were taken at 0.2-μm intervals from the top to the bottom of the acinus on a spinning disk confocal microscope as described above. The number of lumina per acinus was quantified by actin staining. In addition, we defined acini with less or equal to 5 cells, which undergo a maximum of 4 cell divisions, as the early stage of acinus formation. Acini with more than 5 cells were defined as acini in a later expansion stage. Matlab was used to generate scatter plots illustrating the number of lumina in acini.

For measuring spindle angles in acini, γ-tubulin staining was used to indicate spindle pole positions, and actin staining was used to indicate the apical lumen. Spindle angles in acini were then measured followed by a previously described method [S11]. For the taxol treatment, cells were seeded and cultured as described above and incubated with taxol-containing medium for an additional 2 hours before performing immunofluorescence staining.

Transmission electron microscopy of mitotic spindle poles

Mitotic cells were collected by mitotic shake-off [S12], and were fixed in 2.5% glutaraldehyde in PBS for 30 minutes. After post-fixation in 1% osmium tetroxide and embedding in SPI-Pon-Araldite, 150-nm sections were cut and examined with a Philips CM10 transmission electron microscope.

Migration assay

Cells were seeded at confluence with the ibidi culture-insert, and then cultured in serum-free conditions for 48 hours. After removing the inserts, cells were fixed at 2 and 6 hours. The percentage of centrosomes that reorient to a position between the nucleus and the leading edge of the cell during migration was calculated as previously described [S13, S14].

Statistics

Statistical difference was evaluated by un-paired, parametric t-test using GraphPad Prism software. A two-tailed p-value< 0.05 was considered significant.

Supplemental References

S1. Dammermann, A., and Merdes, A. (2002). Assembly of centrosomal proteins and microtubule organization depends on PCM-1. J. Cell Biol. *159*, 255–266.

S2. Hehnly, H., Chen, C. T., Powers, C. M., Liu, H. L., and Doxsey, S. (2012). The centrosome regulates the Rab11- dependent recycling endosome pathway at appendages of the mother centriole. Curr. Biol. *22*, 1944–1950.

S3. Soung, N.-K., Kang, Y. H., Kim, K., Kamijo, K., Yoon, H., Seong, Y.-S., Kuo, Y.-L., Miki, T., Kim, S. R., Kuriyama, R., et al. (2006). Requirement of hCenexin for proper mitotic functions of polo-like kinase 1 at the centrosomes. Mol. Cell. Biol. *26*, 8316–8335.

S4. Chen, C.-T., Hehnly, H., Yu, Q., Farkas, D., Zheng, G., Redick, S. D., Hung, H.-F., Samtani, R., Jurczyk, A., Akbarian, S., et al. (2014). A Unique Set of Centrosome Proteins Requires Pericentrin for Spindle-Pole Localization and Spindle Orientation. Curr. Biol. *24*, 2327–2334.

S5. Delaval, B., Bright, A., Lawson, N. D., and Doxsey, S. (2011). The cilia protein IFT88 is required for spindle orientation in mitosis. Nat. Cell Biol. *13*, 461–468.

S6. Hehnly, H., and Doxsey, S. (2014). Rab11 endosomes contribute to mitotic spindle organization and orientation. Dev. Cell *28*, 497–507.

S7. Blomberg-Wirschell, M., and Doxsey, S. J. (1998). Rapid isolation of centrosomes. Methods Enzymol. *298*, 228–238.

S8. Hung, H.-F., Hehnly, H., and Doxsey, S. (2015). Methods to analyze novel liaisons between endosomes and centrosomes. Methods Cell Biol. *130*, 47–58.

S9. Stout, J. R., Yount, A. L., Powers, J. a, Leblanc, C., Ems-McClung, S. C., and Walczak, C. E. (2011). Kif18B interacts with EB1 and controls astral microtubule length during mitosis. Mol. Biol. Cell *22*, 3070–3080.

S10. Debnath, J., Muthuswamy, S. K., and Brugge, J. S. (2003). Morphogenesis and oncogenesis of MCF-10A mammary epithelial acini grown in three-dimensional basement membrane cultures. Methods *30*, 256–268.

S11. Durgan, J., Kaji, N., Jin, D., and Hall, A. (2011). Par6B and atypical PKC regulate mitotic spindle orientation during epithelial morphogenesis. J. Biol. Chem. *286*, 12461–12474.

S12. Fox, M. H. (2004). Methods for synchronizing mammalian cells. Methods Mol. Biol. *241*, 11–16.

S13. Schliwa, M., and Honer, B. (1993). Microtubules, centrosomes and intermediate filaments in directed cell movement. Trends Cell Biol. *3*, 377–380.

S14. Gomes, E. R., and Gundersen, G. G. (2006). Real-time centrosome reorientation during fibroblast migration. Methods Enzymol. *406*, 579–592.